sustainability

MDPI

Article

Adsorption Potential and Mechanism of Sludge-Based Activated Carbon Modified with Fly Ash for Removal of Heavy Metals

Lixin Mao [1,2], Meng Wu [2,3], Shifei Zhu [1,2,*], Xinfu Wang [2], Jing Zhang [2] and Yunhu Qin [2]

[1] Anhui Provincial Institute of Modern Coal Processing Technology, Anhui University of Science and Technology, Huainan 230051, China
[2] Jiangsu Mineral Resources and Geological Design and Research Institute, China National Administration of Coal Geology, Xuzhou 221006, China
[3] Key Laboratory of Coalbed Methane Resources and Reservoir Formation Process, Ministry of Education, China University of Mining and Technology, Xuzhou 221116, China
* Correspondence: shfzhu@163.com

Abstract: The treatment of sludge has received a lot of attention due to its intractable status and potential resource value. In order to explore methods of sludge resource utilization and to reduce the harm of heavy metals in municipal sewage, this study analyzed the preparation method of a modified sludge adsorbent (MSA). Another common waste (fly ash) was added to raw domestic sludge (RDS) in a certain proportion and developed to have the ability to adsorb heavy metals through multiple steps such as drying, mixing, activation and carbonization. The adsorption performance of the modified sludge adsorbent (MSA) was verified by simulating wastewater containing Cu^{2+} and Cd^{2+}, and the surface and structural properties were studied from a microscopic perspective with the aid of SEM and XRD. This study showed that the MSA was characterized by increased microporosity, an enlarged surface area and enhanced activity of functional groups, and the best performance for heavy metal adsorption was found when the RDS was mixed with fly ash at a ratio of 4:3 and a pH of 8. The highest removal rates for the heavy metals Cu^{2+} and Cd^{2+} were 99.6% and 99.7%, respectively. The adsorption kinetics and adsorption isotherms indicated that the adsorption behavior of the MSA was controlled by both physical and chemical adsorption, and the best fit of the Langmuir adsorption isotherm model revealed the predominance of monolayer adsorption. The present study is a meaningful exploration of the resource utilization of sludge and fly ash and can provide a cheaper and more effective material for addressing heavy metal pollution in domestic sewage.

Keywords: domestic sludge; fly ash; Cu^{2+}; Cd^{2+}; adsorption mechanism

Citation: Mao, L.; Wu, M.; Zhu, S.; Wang, X.; Zhang, J.; Qin, Y. Adsorption Potential and Mechanism of Sludge-Based Activated Carbon Modified with Fly Ash for Removal of Heavy Metals. *Sustainability* **2024**, *16*, 2972. https://doi.org/10.3390/su16072972

Academic Editor: Agostina Chiavola

Received: 22 February 2024
Revised: 22 March 2024
Accepted: 27 March 2024
Published: 3 April 2024

1. Introduction

Sewage, particularly from industrial sources, is laden with substantial quantities of heavy metals like Cu, Pb, Cd and Zn. The release of these metals is on the rise, in parallel with population growth and rapid urbanization [1–5]. Untreated wastewater containing heavy metals discharged into the natural environment can enter the human body through various means such as water, crops and air, thus causing a variety of diseases that are harmful to human health [6–8]. Similar to sewage, sludge from wastewater treatment processes is also of significant concern to scientists, public health officials, waste managers and environmental policy makers, as it contains high levels of various contaminants such as antibiotics, heavy metals and pathogens [9]. Landfills are the most conventional method of disposing of sewage sludge; however, they use a lot of land and there is a risk of contaminating the soil [10]. Sludge incineration is effective in killing pathogens due to the high temperatures used, but it releases hazardous substances such as heavy metals [2], and dioxins and furans [11] may develop during the process. With the accelerating rate of resource consumption (such as agricultural fertilizers) [12] and the emphasis on ecology [13], the use of sludge as a resource is becoming increasingly popular. Sludge has shown

great promise as an agricultural fertilizer and a soil conditioner [14] and for extracting animal feed [15] with high contents of organic matter, N and P. However, the heavy metals contained in the sludge limit the resource utilization of the sludge [16].

Given the safety risks associated with the above methods of sludge disposal, such as landfilling, incineration or using sludge to treat agricultural fertilizer, it is necessary to develop a safer way of disposing of sludge. According to the concept of using waste to treat waste, the use of sludge-modified materials to absorb heavy metals in sewage may be the best of both worlds, as it can reduce the heavy metal pollution of sewage and achieve the reuse of sludge. Equally importantly, sewage treatment plants are a source of greenhouse gas emissions that cannot be ignored [17], and their carbon emissions account for 1% to 2% of the total social carbon emissions [18]. Therefore, the use of waste (sludge) in the process of sewage treatment to reduce resource consumption has a positive effect on the realization of "carbon neutrality" goals. An increasing amount of research has focused on the potential of sludge as a sorbent. The adsorption performance of the sludge as biochar was optimized by adjusting the temperature [19,20], pH [21,22], adsorption time [23] and activator concentration [24] for the treatment of industrial wastewater. Devi and Saroha (2016) [25] reviewed some studies on the addition of various additives (agricultural residues, industrial wastes and metals) to sludge to enhance the adsorption performance of the adsorbent.

Improper disposal of fly ash containing high concentrations of heavy metals akin to sludge generated by factories and thermal power plants worldwide can result in soil degradation and pose significant risks to human health and the environment [26–28]. The main resource-based utilization of fly ash is in road infrastructure and construction materials [29], soil conditioners [30,31], the ceramics industry [32] and catalysts [33,34]. Fly ash, which has a large specific surface area and a large number of active sites, can undergo chemisorption and physical adsorption with the adsorbent. Therefore, fly ash is also often used as an adsorbent to remove metal ions [35,36] and organic pollutants [37,38].

It should be noted that many studies have used sludge or fly ash as heavy metal adsorption materials. However, few studies have reported the similarities and differences between the two kinds of solid wastes in terms of the adsorption capacity of heavy metals. Whether combining the complementary advantages of the two solid wastes in physical adsorption or chemisorption characteristics can further improve the adsorption capacity of heavy metals is a significant question in terms of using waste to treat waste. The current study investigates the viability of using these two substances as activated carbon materials based on an analysis of their fundamental properties. The adsorption potential of this material was tested using simulated industrial wastewater containing heavy metals. The aim is to realize the resourceful use of sludge and fly ash, as well as to provide a new material to address heavy metal pollution in industrial wastewater.

2. Materials and Methods

2.1. Sources of Sludge and Fly Ash

Jiangsu Province is one of the most economically developed provinces in China. Its economic development is accompanied by a large amount of urban sewage (including domestic sewage and industrial wastewater) and the resulting sludge, with an output of about 5 billion tons/year and 1.1 million tons/year, respectively, ranking top among all provinces in the country (Figure 1). The production scale of fly ash in Jiangsu Province is also large, which is related to the relatively large proportion of thermal power generation, which is 14 to 21 percentage points higher than the national average in the same period. Based on the relationship between coal burning and fly ash production, it is expected that fly ash production exceeded 65 million tons in 2021 alone [39].

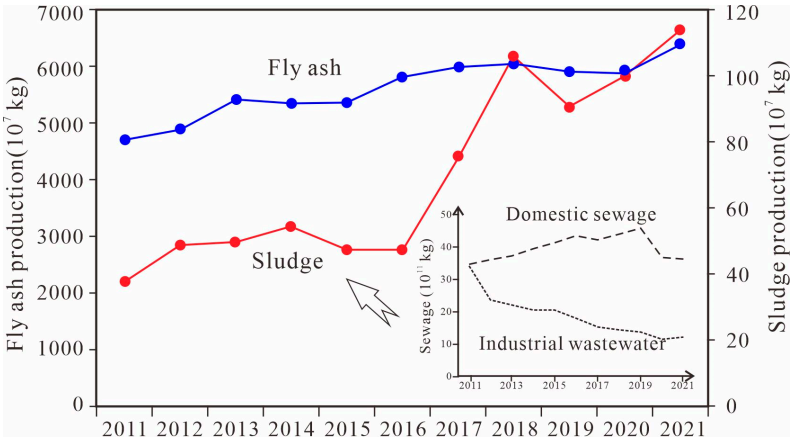

Figure 1. Production of sewage, sludge and fly ash in Jiangsu Province.

In our study, fly ash and sludge samples were obtained from a power plant and sewage treatment plants in Jiangsu Province. Among them, the sludge samples included sludge from a domestic sewage treatment plant (DSS) and sludge from an industrial wastewater treatment plant (IWS). As shown in Figure 1, the output of domestic sewage in Jiangsu Province is higher than that of industrial wastewater. Therefore, this study focuses on a GZ domestic sewage treatment plant, where an A/O (anaerobic oxygen) process is adopted. The design scale is 100,000 tons/day, and the effluent quality is Class I A standard.

All fly ash and sludge samples were homogenized, dried at 105 °C for 24 h and then ground to 200 mesh. To study the characteristics of sludge samples, the pH, total phosphorus, available phosphorus and organic matter were tested. The pretreatment sludge samples were mixed with 0.01 mol/L $CaCl_2$ solution, and then their pH values were determined by a pH meter (PHS-3C). The contents of total phosphorus and available phosphorus in the sludge samples were determined after the leaching of phosphate minerals and organophosphorus compounds. The content of organic matter in the sludge was determined by a high-frequency infrared carbon sulfur analyzer (HCS-801A). The pretreatment and the following experiments were completed at the CNACG (the China National Administration of Coal Geology) Key Laboratory of Mineral Resource in Coal Measures.

2.2. Preparation of Modified Sludge Adsorbent (MSA)

All raw domestic sludge (RDS) used in the follow-up experiment was from the GZ domestic sewage treatment plant. First, 900 g of RDS was divided equally into 5 groups, numbered 1 to 5. Then, the fly ash sample was dried and added to the above groups numbered 2, 3, 4 and 5 in the proportions 4:1, 4:2, 4:3 and 4:4, respectively. Group 1 was used as a blank control without adding fly ash. The samples of each of the five groups were mixed well and ground.

The mixture of $ZnCl_2$ and H_2SO_4 facilitates dehydration, condensation and swelling reactions, resulting in a carbon adsorbent with a high adsorption capacity [40]. The adsorption capacity of the adsorbent increases with increasing $ZnCl_2$ up to a certain concentration (3 mol/L), and further increasing concentrations of $ZnCl_2$ lead to a decrease in adsorption capacity [24]. The $ZnCl_2$ solution (3 mol/L) was prepared with sulfuric acid (98%) in a 10:1 ratio by volume. The prepared activator was added to the 5 groups of samples at a solid mass to liquid volume ratio of 1:4. The solid product was dried at 105 °C for 24 h after the suspension had been left at 100 rpm for 24 h and then heated to 700 °C in a high-temperature tube furnace at a slope of 10 °C/min.

A high inorganic content clogs the pores of a sludge-based adsorbent, thus preventing the development of the surface area and porosity, leading to a reduction in the adsorption capacity of the adsorbent [23–25]. Washing sludge-based activated carbon with HCl can greatly improve the pore volume [41,42]. The samples were washed three times in sequence with HCl (3 mol/L) and hot distilled water (70–80 °C). The modified material was stored

in a desiccator and the samples were dried at 105 °C for 24 h before being crushed to a size of less than 200 mesh (Figure 2).

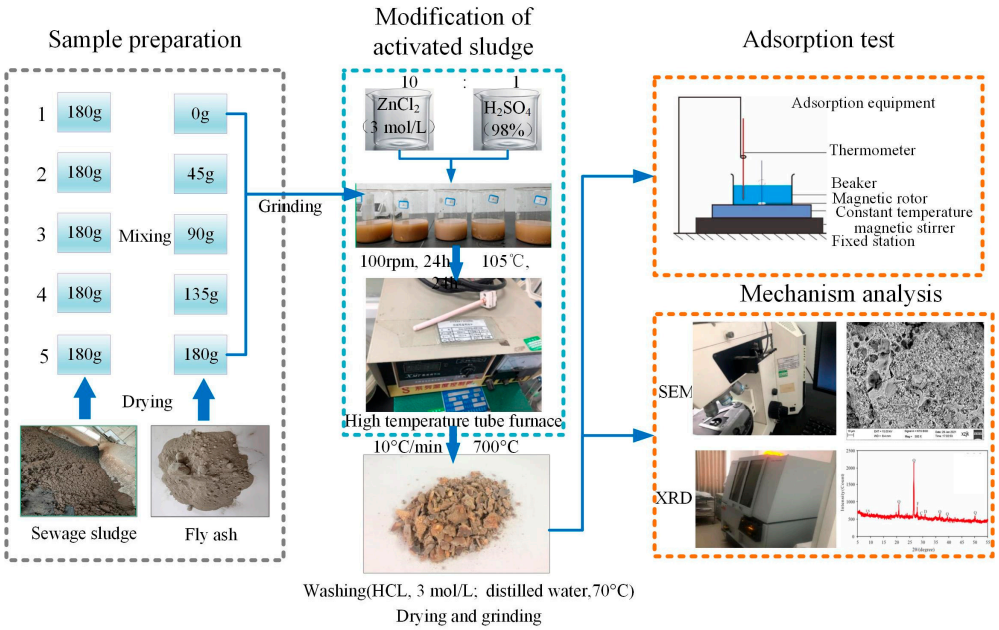

Figure 2. Flow chart of sludge-based activated carbon preparation and mechanism analysis. Sludge and fly ash were mixed in different proportions. Activated carbon was prepared from the activated mixture under specific conditions (700 °C). Activated carbon was used to verify the adsorption capacity and adsorption mechanism of heavy metal ions (Cu^{2+} and Cd^{2+}).

2.3. Characteristics of Modified Samples

2.3.1. Adsorption of Heavy Metals

In order to quantitatively calculate the adsorption characteristics of heavy metals by the MSA, consistent amounts of the MSA were used in all experiments based on the solid-liquid ratio employed in similar studies conducted by previous researchers [8,16]. The above MSA samples containing different proportions of fly ash numbered 1 to 5 were each weighed to 2 g. A solution containing Cu^{2+} and Cd^{2+} ions was prepared, according to the concentration of heavy metals in local municipal sewage, to test the adsorption capacity of the MSA for heavy metals. Different MSA materials and the same concentration of the simulated wastewater solution (500 mL) were added in six sets of experiments (one blank experiment). The samples were stirred in a magnetic stirrer at 100 r/min for 2 h. The concentration of Cu^{2+} and Cd^{2+} in the supernatant of the centrifuged solution was determined after adjusting the pH of the solution to 7 with NaOH and HNO_3.

Some experiments were carried out to investigate the influencing factors and adsorption mechanisms of the MSA4 samples. MSA4 samples of equal mass were added to simulated wastewater with different pH values, and the pH values of the simulated wastewater solutions were adjusted to 2, 4, 6, 8 and 10. At the same time, another set of experiments was carried out at room temperature and pH 5. Five beakers were added with simulated wastewater with different Cu^{2+} and Cd^{2+} contents, and the concentrations of Cu^{2+} and Cd^{2+} were set at 30 mg/L, 60 mg/L, 90 mg/L, 120 mg/L and 180 mg/L. A sample of 2 g MSA4 was then added to each of the five beakers. In the above experiments, the MSA was mixed with wastewater and placed in a 120 r/min magnetic stirrer, and the supernatant after centrifugation was taken to determine the concentration of Cu^{2+} and Cd^{2+}.

Each experiment was repeated three times, and additional analysis was performed when the difference between the two measurements was greater than 5%. The determination of the concentration is based on the standards "Water quality—Determination of 65 elements—Inductively coupled plasma-mass spectrometry" (HJ 700-2014) and "Wa-

ter quality—Determination of 32 elements—Inductively coupled plasma optical emission spectrometry"(HJ 776-2015).

2.3.2. Characterization of Physical and Chemical Properties

The RDS, fly ash and MSA were selected to observe their microscopic characteristics. The content of chemical elements in the samples was analyzed by energy-dispersive X-ray spectroscopy (EDS), and the surface microscopic morphology of the samples was analyzed by scanning electron microscopy (SEM). SEM with an energy spectrum can quickly and accurately obtain the morphology, structural characteristics and composition information of samples, and has a wide range of applications in the microscopic characterization of fly ash [43] and modified sludge.

2.3.3. Data Calculation

The adsorption amount Q_e (mg/g) of the MSA material and the removal rate W (%) of heavy metals were calculated by the following formulas, respectively.

$$Q_e = (C_0 - C_e)\mathrm{V}/(1000\mathrm{M}) \quad (1)$$

$$W = (C_0 - C_e)/C_0 100\% \quad (2)$$

where C_0 (mg/g) and C_e (mg/L) are the initial concentration of the ions to be tested and the concentration at adsorption equilibrium, respectively, V (mL) is the volume of the simulated wastewater solution and M (g) is the MSA material added quality.

3. Results

3.1. Properties of Sludge

3.1.1. Chemical Characteristics

The contents of pH, total phosphorus, available phosphorus, organic matter and major heavy metals in the sludge samples were analyzed, and the results are presented in Table 1. The pH values of the sludge samples are 7.15 and 8.50. The contents of total phosphorus, available phosphorus and organic matter in the DSS are 12,620 mg/kg, 236 mg/kg and 25.29%, respectively, which are higher than those in the IWS. It can be seen that the DSS contains more nutrients needed for plant growth, indicating a better application prospect in agricultural soil.

Table 1. The main physical and chemical properties of different sludges collected from Jiangsu Province.

Parameter	Sludge Types		Unit
	DSS	IWS	
pH	7.15	8.50	\
Tp	12,620	278	mg/kg
Ap	236	194	mg/kg
Om	25.29	2.89	%
Cu	77.5	8.16	μg/g
Cr	143	60.8	μg/g
Zn	1344	141	μg/g
Cd	3.87	0.21	μg/g
Pb	32.8	6.70	μg/g
Mn	294	2648	μg/g
Ni	43.2	42.9	μg/g

Note: Data are shown as their replicate mean. Tp: total phosphorus; Ap: available phosphorus; Om: organic matter.

The heavy metals (Cu, Cr, Zn, Cd, Pb, etc.) and inorganic salts (Si, Na, Al, Ca and P) constitute the ash content of the adsorbent. As shown in Table 1, the content of heavy metals in the DSS is higher than that in the IWS on the whole, except the Mn element. Studies have shown that a high ash content of an adsorbent is shown as inert materials,

which does not affect the porosity [44] and even improves the adsorption capacity of metal ions on sludge-based adsorbents [45]. Moreover, the output of the DDS is much higher than the IWS in Jiangsu Province. In order to improve the adsorption capacity of adsorbents and facilitate further popularization and application, the DDS is selected as the raw material of the modified adsorbent.

3.1.2. Microstructure and Composition

The microstructure of the RDS needs to be observed to clarify the changes in the modification process. Figure 3 shows the SEM images and the elemental composition of the RDS determined by an energy-dispersive spectrometer. The RDS is characterized by a rough surface, poor sorting and a large particle size range. The overall porosity is low, and the pore type is dominated by intergranular pores, especially between large particles and small particles. Intergranular pores are not developed because the well-crystalline phase is found to be absent. Particle surface cracks are not developed, and there are only a small number of microcracks. Generally, the RDS has a compact structure and small surface area.

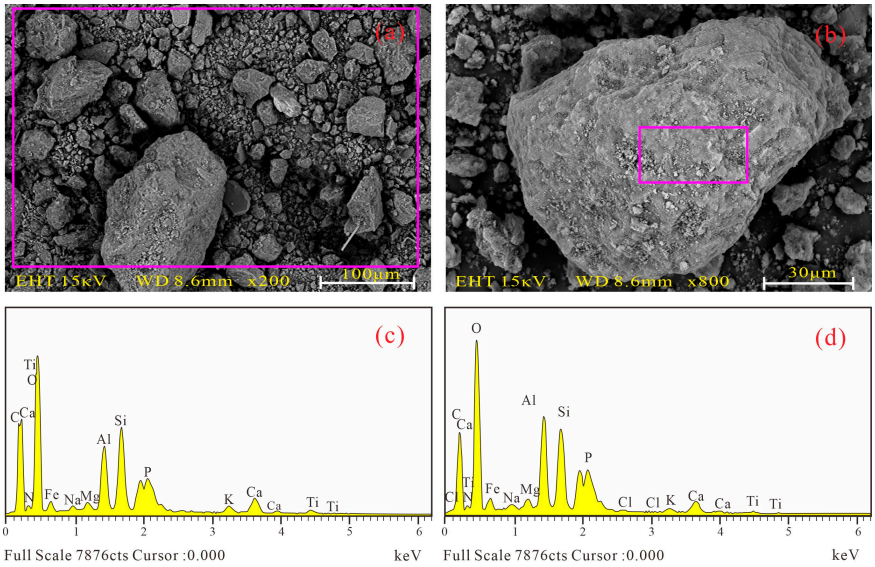

Figure 3. Microscopic features and elemental content of RDS. (**a**) Overall vision, ×200; (**b**) partial vision, ×800; (**c**) elemental content of (**a**); (**d**) elemental content of (**b**).

The energy-dispersive spectrum revealed the elemental content of the RDS. The weight percentages and atomic percentages of each element were calculated separately. The elements with the highest weight percentages were carbon (C, 38.5%), oxygen (O, 42.9%), silicon (Si, 6.1%), Ferrum (Fe, 7.5%) and aluminum (Al,4.3%), indicating that the RDS contained high levels of $CaCO_3$, SiO_2, Fe and Al_2O_3.

3.2. Properties of Fly Ash

Scanning electron microscopy at different magnifications revealed that fly ash has a rough surface (Figure 4). On the particle surfaces, numerous micropores less than 10 μm in size are evident. These significantly enhance the surface area and porosity of the fly ash, which are crucial factors for the adsorption of pollutants on the adsorbent surface. With the analysis of the EDS and XRD combined, it was found that the mineral composition of the fly ash is dominated by quartz, feldspar, calcite and illite/smectite mixed layers, followed by minor amounts of rhodochrosite, pyrite, barite and mullite.

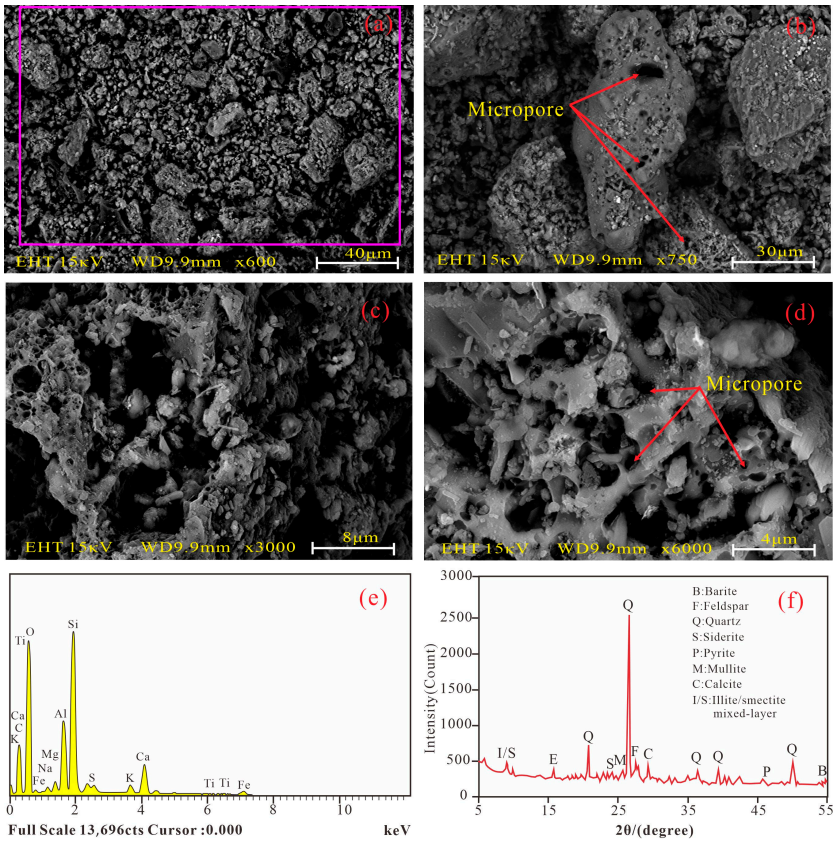

Figure 4. Microscopic features, elemental content and mineral composition of fly ash. (**a**–**d**) The magnification increases sequentially, abundant micropores, ×600, ×750, ×3000, ×6000; (**e**) elemental content of (**a**); (**f**) mineral composition of the entire sample.

3.3. Adsorption Experiment Results

The MSA modified with different proportions of fly ash with different adsorption efficiencies of Cu^{2+} and Cd^{2+} was studied by adding simulated wastewater mixed with Cu^{2+} and Cd^{2+}. As shown in Figure 5, the adsorption efficiency of the MSA for Cu^{2+} and Cd^{2+} is different, and the adsorption of Cu^{2+} is greater than that of Cd^{2+}, indicating the difference in the adsorption capacity of the MSA for different heavy metals. The removal rates of Cu^{2+} and Cd^{2+} by the MSA were 93.8%~98.6% (mean 96.1%) and 24.5%~40.0% (mean 34.3%), respectively. The content of fly ash in MSA1~MSA5 increased gradually, which affected the adsorption capacity of the MSA for heavy metals. Moreover, MSA4 had the highest removal rates of Cu^{2+} and Cd^{2+}, showing the best adsorption capacity among the five MSA samples.

Adsorption tests of MSA4 were carried out in simulated wastewater solutions with pH values of 2, 4, 6, 8 and 10. As shown in Figure 6, when the pH value increased from 2 to 8, the removal rates of Cu^{2+} and Cd^{2+} by MSA4 increased from 8.2% to 99.6% and from 3.1% to 99.0%, respectively. The results showed that the sludge-modified materials were extremely unattractive for adsorption in acidic solutions and significantly better in alkaline environments than in acidic environments. An excessively high alkaline environment had little effect on the adsorption of Cd^{2+}, but the adsorption performance for Cu^{2+} was significantly reduced. The highest removal of Cu^{2+} and Cd^{2+} by MSA4 was achieved when the pH values were 8 and 10, reaching 99.6% and 99.7%, respectively.

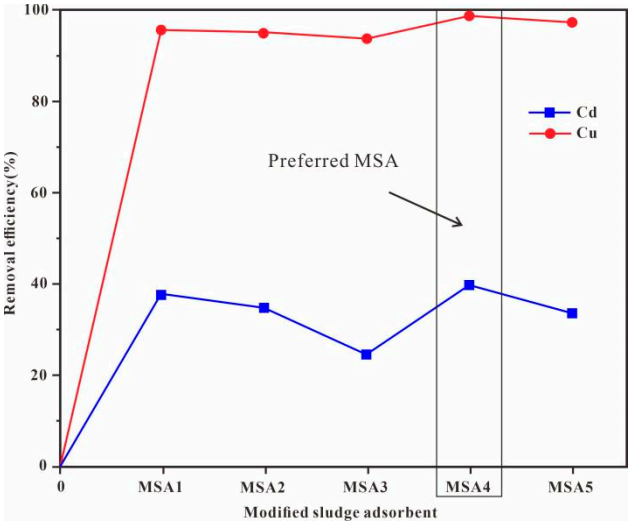

Figure 5. Removal rates of Cu^{2+} and Cd^{2+} by MSA modified with different proportions of fly ash.

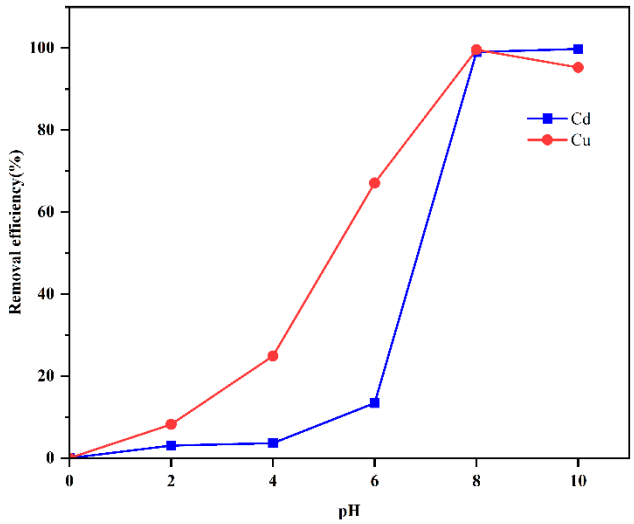

Figure 6. Adsorption rate of MSA4 at different pH values, indicating a higher removal rate in alkaline solution than that in acidic condition.

4. Discussion

4.1. Influence of Fly Ash Content and pH

The adsorption capacity of the MSA for Cu^{2+} and Cd^{2+} can be improved by the amount of fly ash added to the MSA material, which is related to the physical and chemical properties of fly ash. The main components of fly ash are SiO_2 and Al_2O_3 (Figure 4), and its Si-O bonds and Al-O bonds are gradually broken due to the chemical interaction with $ZnCl_2$ and H_2SO_4 and other physical effects such as high temperature and grinding during the transformation process (Figure 2). These increase the adsorption sites of the MSA for Cu^{2+} and Cd^{2+}. In addition, the large specific surface area, partial carbon and active sites of fly ash further enhance the adsorption capacity of the MSA for Cu^{2+} and Cd^{2+}.

The pH value of the solution can significantly influence the adsorption capacity of the adsorbent [46,47]. The adsorption capacity of MSA4 for Cu^{2+} and Cd^{2+} increased with the increase in pH value (Figure 6). The main reason may be that the increase in pH led to a decrease in the H^+ concentration in the reaction system, which promoted the binding of the groups in the MSA (-OH and $-NH_2$) to Cu^{2+} and Cd^{2+}. On the contrary, the presence of large amounts of H^+ in acidic solutions changes the charge distribution on the surface of the modified sludge. The enhanced electrostatic repulsion of the modified

sludge is due to the increase in the positive charge. The abundance of H^+ in the solution competes with Cu^{2+} and Cd^{2+} for the limited sorption sites and thus reduces its sorption. The OH^- present in alkaline solutions reacts with Cu^{2+} and Cd^{2+} to form hydroxide or carbonate precipitates [48]. Therefore, a pH that is too high has little effect on increasing the adsorption capacity of the MSA for Cu^{2+} and Cd^{2+}.

4.2. Micro Components and Structure

MSA4 was tested by SEM, EDS and XRD (Figure 7). The results showed that the smaller particle size of both resulted in an increased surface area and more developed microporosity (<10 μm), which may increase the contact area between MSA4 and Cu^{2+} and Cd^{2+} in solution to some extent and thus improve the adsorption [46]. The better absorbing MSA4 sample has a larger surface area, more micropores and more filamentous or fluffy minerals compared to the RDS and fly ash, which confirms the above explanation (Figures 3, 4 and 7).

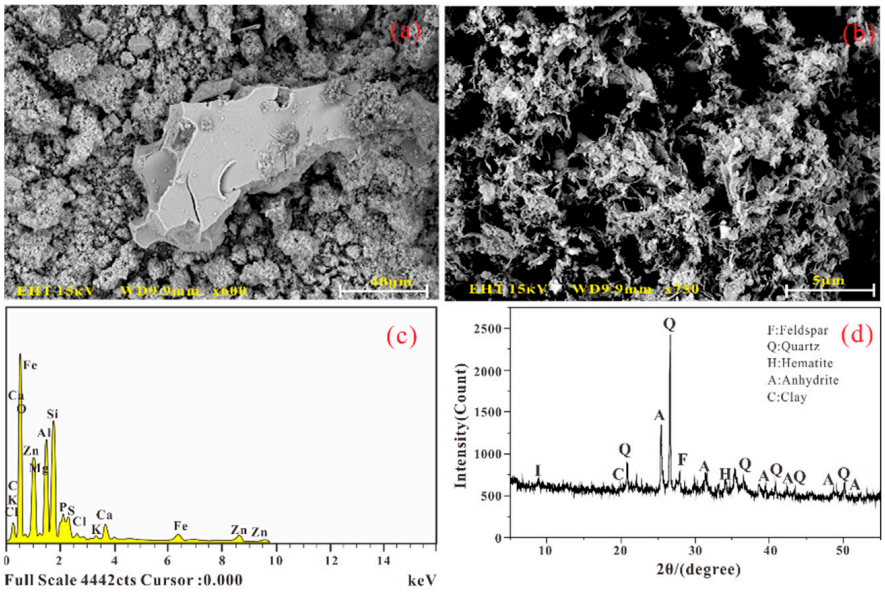

Figure 7. Microscopic features, elemental content and mineral composition of MSA4. (**a**), (**b**) SEM image, ×600, ×750; (**c**) elemental content of (**a**); (**d**) mineral composition of the entire sample.

Furthermore, the elemental composition of the MSA4 sample was confirmed to have undergone changes as revealed by EDS and XRD analysis. The atomic percentages of oxygen (O), silicon (Si), aluminum (Al) and calcium (Ca) exhibited increases, while carbon (C) showed a decrease. Notably, significant alterations were observed in the mineral composition of MSA4, with quartz, feldspar and hard gypsum being predominant, followed by clay minerals and hematite. Ultimately, these changes influenced the functional group activity, exchangeable ions and charge distribution on the surface of MSA4, thereby impacting its adsorption [49,50].

4.3. Adsorption Mechanism

4.3.1. Adsorption Kinetic

The adsorption experimental conditions were determined through pre-experiments, and representative experimental conditions were selected for kinetic adsorption experiments. The experimental results of the adsorption of Cu^{2+} and Cd^{2+} on the MSA were fitted by a pseudo-first-order kinetic equation, a pseudo-second-order kinetic equation and an intragranular diffusion equation. The kinetic equations are expressed as follows:

pseudo-first-order kinetic equation:

$$Q_t = Q_e\left(1 - e^{-k_1 t}\right) \quad (3)$$

pseudo-second-order kinetic equation:

$$Q_t = \frac{Q_e^2 k_2 t}{1 + Q_e k_2 t} \tag{4}$$

intragranular diffusion equation:

$$Q_t = K_{id} t^{1/2} + C \tag{5}$$

where Q_t and Q_e are the adsorption amounts of Cu^{2+} and Cd^{2+} by the MSA at time t and the adsorption equilibrium, respectively, $mg \cdot g^{-1}$; t is the adsorption time, min; and k_1, k_2 and k_{id} are the rate constants of the pseudo-first-order, pseudo-second-order and intraparticle diffusion model, in units of h^{-1}, $mg \cdot (g \cdot h)^{-1}$ and $mg \cdot (g \cdot h^{0.5})^{-1}$, respectively.

In general, the pseudo-first-order kinetic equation, pseudo-second-order kinetic equation and intraparticle diffusion equation exhibit superior efficacy in simulating the adsorption kinetics process. Figure 8 shows the variation in the adsorption amount of Cu^{2+} and Cd^{2+} on MSA4 with time and the fitting of different kinetic curves. It can be seen from the figure that the adsorption of MSA4 is faster before 150 min, and it tends toward equilibrium at 350 min. The pseudo-first-order kinetics can reflect the initial adsorption process of Cu^{2+} and Cd^{2+} by MSA4, indicating that the initial adsorption is mainly controlled by diffusion [51]. The main factor of pseudo-second-order kinetic adsorption is chemical bond formation, indicating that chemisorption is dominant [52]. The intraparticle diffusion kinetics curve did not intersect the origin, suggesting that the adsorption process involves a combination of multiple adsorption mechanisms.

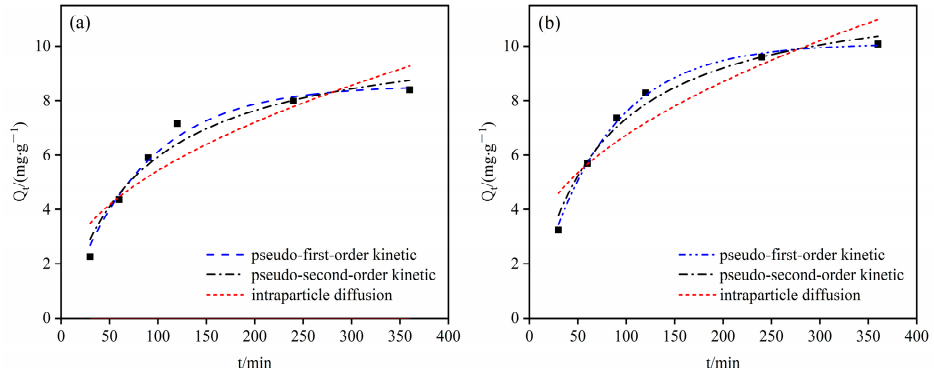

Figure 8. The adsorption kinetics of Cd^{2+} (**a**) and Cu^{2+} (**b**) on MSA4. The adsorption capacity as a function of the adsorption duration and fitting results based on the three adsorption kinetic models.

4.3.2. Adsorption Isotherm

Langmuir and Freundlic adsorption isotherm equations were used to describe the adsorption process of Cu^{2+} and Cd^{2+} by MSA4.

Langmuir equation:

$$Q_e = \frac{K_L Q_m C_e}{1 + K_L C_e} \tag{6}$$

Freundlich equation:

$$Q_e = K_f C_e^{\frac{1}{n}} \tag{7}$$

where Q_e is the adsorption capacity of Cu^{2+} and Cd^{2+} at the adsorption equilibrium, $mg \cdot g^{-1}$; K_L is the Langmuir characteristic adsorption constant, $L \cdot g^{-1}$; Q_m is the maximum adsorption capacity, $mg \cdot g^{-1}$; C_e is the concentration of Cu^{2+} and Cd^{2+} at the adsorption equilibrium, $mg \cdot L^{-1}$; K_f is the Freundlich adsorption capacity parameter; and n is the Freundlich index.

The isotherms for the adsorption of Cu^{2+} and Cd^{2+} by MSA4 (Figure 9) were simulated with the widely used Langmuir and Freundlich equations (the corresponding parameters

are summarized in Table 2). The R^2 of the adsorption isotherms for Cu^{2+} and Cd^{2+} in the Langmuir model are 0.9972 and 0.982, respectively, which are higher than 0.9323 and 0.9526 in the Freundlich model. Therefore, the adsorption isotherms of Cu^{2+} and Cd^{2+} fit better with Langmuir equations. The Cu^{2+} and Cd^{2+} adsorption isotherms of MSA4 also showed the greatest adsorption capacity at the same equilibrium concentrations in the solution and had their greatest slope at the low concentrations. The maximum adsorption capacities of MSA4 for Cu^{2+} and Cd^{2+} at room temperature are 11.34 mg/g and 10.68 mg/g (Table 2), respectively, indicating that MSA4 has a better adsorption capacity for Cu^{2+}. In addition, compared with the sorption isotherm of Cu^{2+}, it was found the Cd^{2+} sorption isotherm was less steep, so the adsorption rate of MSA4 on Cu^{2+} is faster.

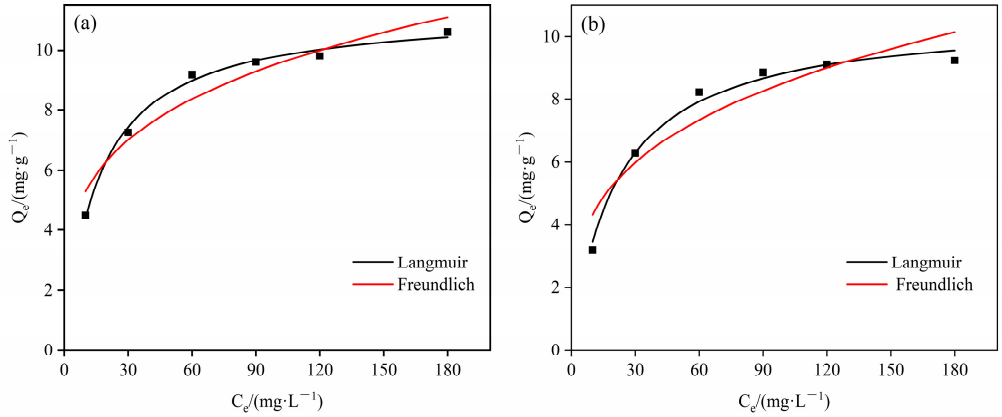

Figure 9. The adsorption isotherms of Cu^{2+} (**a**) and Cd^{2+} (**b**) on MSA4. The equilibrium Cu^{2+} and Cd^{2+} adsorption capacity as a function of the initial Cu^{2+} and Cd^{2+} concentration and fitting results based on the Langmuir model and the Freundlich model.

Table 2. Isotherm modeling parameters for adsorption of Cd^{2+} and Cu^{2+} on MSA4.

Metal Ions	Adsorption Isotherm	Fitting Equations	Parameter 1	Parameter 2	R^2
Cd^{2+}	Langmuir	$Q_e = 0.5104C_e/(1 + 0.0478C_e)$	Q_m = 10.6778	K_L = 0.0478	0.9820
	Freundlich	$Q_e = 2.1973\ C_e^{0.2945}$	K_f = 2.1973	1/n = 0.2945	0.9562
Cu^{2+}	Langmuir	$Q_e = 0.7193C_e/(1 + 0.0634C_e)$	Q_m = 11.3439	K_L = 0.0634	0.9972
	Freundlich	$Q_e = 2.9243\ C_e^{0.2568}$	K_f = 2.9243	1/n = 0.2568	0.9323

Note: The meaning and unit of the parameters in the table are given in the formula.

4.3.3. Metal Sorption Behavior

The adsorption kinetic curves and adsorption isotherms of MSA4 for Cu^{2+} and Cd^{2+} reveal the complexity of its adsorption behavior. The adsorption processes controlled by diffusion-controlled and chemisorption mechanisms play different roles in different stages of adsorption. The fitting effects of the Langmuir and Freundlic adsorption isotherm models for the adsorption of Cu^{2+} and Cd^{2+} by MSA4 indicate that both monolayer and multilayer adsorption work on homogeneous surfaces. Among them, the Langmuir model with the best fitting effect shows that monolayer adsorption is the most important adsorption behavior.

Considering the excellent fitting effects of the pseudo-second-order kinetic model and the Langmuir isotherm model on the MSA adsorption process, it can be inferred that the MSA exhibits a strong chemical adsorption capacity for Cu^{2+} and Cd^{2+} [16,52]. Therefore, it is speculated that there exist abundant hydroxyl and carboxyl functional groups on the surface of MSA4, which interact with Cu^{2+} and Cd^{2+} to form surface complexes [9]. MSA4 contains a large amount of exchangeable cations such as Ca^{2+}, which is easily ion-exchanged with Cu^{2+} and Cd^{2+} to release Ca^{2+} and absorb Cu^{2+} and Cd^{2+} [53]. Chen

et al. [54] prepared sludge biochar by anaerobic pyrolysis at 900 °C to reach a maximum adsorption of (42.80 ± 2.38) mg/g, and when the solution system pH value was greater than 10.17, the surface of the biochar was negatively charged and showed strong electrostatic adsorption of positively charged Cu^{2+} and Cd^{2+}. This was similar to the present study, in which MSA4 had the maximum adsorption in an alkaline environment. In addition, surface precipitation under alkaline conditions is an important adsorption behavior [55].

5. Conclusions

The MSA was prepared using chemical reagents, high-temperature activation and other physical and chemical methods, employing sludge and fly ash as raw materials. The incorporation of fly ash into the sludge resulted in a refined pore structure, increased surface area and an enhanced presence of active functional groups. When the mass ratio of domestic sludge to fly ash was 4:3, the MSA exhibited optimal adsorption capacity for Cu^{2+} and Cd^{2+}. Moreover, an alkaline environment facilitated the removal efficiency of heavy metals from simulated wastewater by MSA4, with maximum removal rates recorded at 99.6% for Cu^{2+} and 99.7% for Cd^{2+}. Additionally, MSA4 demonstrated a maximum adsorption capacity of 11.34 mg/g for Cu^{2+} and 10.68 mg/g for Cd^{2+}. Considering the adsorption capacity and adsorption rate, MSA4 has better adsorption performance for Cu^{2+}. An adsorption kinetics analysis along with isotherm modeling revealed that MSA4 exhibited a combination of physical and chemical adsorption mechanisms, with the Langmuir monolayer model providing the best fit to describe its predominant behavior. Consequently, MSA4 can be considered for the treatment of sewage containing heavy metals to achieve the purpose of simultaneously treating sewage, sludge, and fly ash.

Author Contributions: L.M.: Conceptualization, Methodology, Writing—Original Draft and Editing. M.W.: Project Administration and Funding Acquisition. S.Z.: Resources and Term. X.W.: Validation and Data Curation. Y.Q.: Supervision and Investigation. J.Z.: Formal Analysis and Visualization. All authors have read and agreed to the published version of the manuscript.

Funding: This research was funded by the Open Research Fund Program of the Anhui Provincial Institute of Modern Coal Processing Technology, Anhui University of Science and Technology (Grant No. MTY202206), the Xuzhou Science and Technology Innovation Special Fund (Grant Nos. KC23073 and KC23120), and the Open Research Fund Program of the Jiangsu Design Institute of Geology for Mineral Resources (Grant No. JSY2020-6).

Institutional Review Board Statement: Not applicable.

Informed Consent Statement: Not applicable.

Data Availability Statement: Data are contained within the article.

Conflicts of Interest: The authors declare no conflicts of interest.

References

1. Poumanyvong, P.; Kaneko, S. Does urbanization lead to less energy use and lower CO_2 emissions? A cross-country analysis. *Ecol. Econ.* **2010**, *70*, 434–444. [CrossRef]
2. Cantinho, P.; Matos, M.; Trancoso, M.A.; dos Santos, M.M.C. Behaviour and fate of metals in urban wastewater treatment plants: A review. *Int. J. Environ. Sci. Technol.* **2015**, *13*, 359–386. [CrossRef]
3. Agoro, M.A.; Adeniji, A.O.; Adefisoye, M.A.; Okoh, O.O. Heavy Metals in Wastewater and Sewage Sludge from Selected Municipal Treatment Plants in Eastern Cape Province, South Africa. *Water* **2020**, *12*, 2746. [CrossRef]
4. Geng, Y.M.; Zhang, C.B.; Zhang, D.D.; Yan, S.X.; Sun, T.F.; Chen, L.; Wang, J.; Mao, Y.X. Speciation and ecological risk assessment of heavy metal (loid)s in the municipal sewage sludge of China. *Environ. Sci.* **2021**, *42*, 4834–4843.
5. Mao, H.; Zhang, Y.; Wang, H.; Cui, K.; Yu, L.; Tan, T. Recycling sewage sludge into ceramic materials: A review. *Environ. Chem. Lett.* **2023**, *21*, 1659–1672. [CrossRef]
6. Cieślik, B.M.; Namieśnik, J.; Konieczka, P. Review of sewage sludge management: Standards, regulations and analytical methods. *J. Clean. Prod.* **2015**, *90*, 1–15. [CrossRef]
7. Rajasulochana, P.; Preethy, V. Comparison on efficiency of various techniques in treatment of waste and sewage water—A comprehensive review. *Resour.-Effic. Technol.* **2016**, *2*, 175–184.

8. Tang, J.; He, J.; Liu, T.; Xin, X. Removal of heavy metals with sequential sludge washing techniques using saponin: Optimization conditions, kinetics, removal effectiveness, binding intensity, mobility and mechanism. *RSC Adv.* **2017**, *7*, 33385–33401. [CrossRef]
9. Singh, S.; Kumar, V.; Dhanjal, D.S.; Datta, S.; Bhatia, D.; Dhiman, J.; Samuel, J.; Prasad, R.; Singh, J. A sustainable paradigm of sewage sludge biochar: Valorization, opportunities, challenges and future prospects. *J. Clean. Prod.* **2020**, *269*, 122259. [CrossRef]
10. Werther, J.; Ogada, T. Sewage sludge combustion. *Prog. Energy Combust. Sci.* **1999**, *25*, 55–116. [CrossRef]
11. Bolzonella, D.; Fatone, F.; Pavan, P.; Cecchi, F. Poly-chlorinated dibenzo-p-dioxins, dibenzo-furans and dioxin-like poly-chlorinated biphenyls occurrence and removal in conventional and membrane activated sludge processes. *Bioresour. Technol.* **2010**, *101*, 9445–9454. [CrossRef]
12. Cao, C.; Zhou, X.T.; Gao, Y.X.; Ma, Z.W.; Wang, Y.; Ying, C.Y.; Xie, J.H.; Zhou, F.H.; Jiang, H.Y.; Ma, Y.H. Effects of partial replacement of chemical fertilizer with sludge compost on maize growth in chromium-contaminatedfarmland. *J. Agro-Environ. Sci.* **2023**, *42*, 2453–2463.
13. Jafaripour, A.; Rowson, N.A.; Ghataora, G.S. Utilisation of residue gas sludge (BOS sludge) for removal of heavy metals from acid mine drainage (AMD). *Int. J. Miner. Process.* **2015**, *144*, 90–96. [CrossRef]
14. Kahiluoto, H.; Kuisma, M.; Ketoja, E.; Salo, T.; Heikkinen, J. Phosphorus in manure and sewage sludge more recyclable than in soluble inorganic fertilizer. *Environ. Sci. Technol.* **2015**, *49*, 2115–2122. [CrossRef] [PubMed]
15. Hwang, J.; Zhang, L.; Seo, S.; Lee, Y.W.; Jahng, D. Protein recovery from excess sludge for its use as animal feed. *Bioresour. Technol.* **2008**, *99*, 8949–8954. [CrossRef]
16. Wu, M.; Wang, X.Q.; Mao, L.X.; Wang, X.F.; Zhu, S.F.; Zhang, G.C.; Xun, N.C.; Qin, Y.H. Experimental study on Cd(II) and Cu(II) of adsorbent prepared by mixing fly ash and domestic sludge. *Appl. Chem. Ind.* **2023**, *52*, 689–696.
17. Du, W.J.; Lu, J.Y.; Hu, Y.R.; Xiao, J.X.; Yang, C.; Wu, J.; Huang, B.C.; Cui, S.; Wang, Y.; Li, W.W. Spatiotemporal pattern of greenhousegas emissions in China's wastewater sector and pathways towardscarbon neutrality. *Nat. Water* **2023**, *1*, 166–175. [CrossRef]
18. Sun, M.; Yang, J.L.; Xiao, P.Y.; Li, J.S.; Wang, Q.B.; Liu, G.; Huo, M.X. Progress and new trend of low carbon and resource recovery technologies for municipal wastewater treatmentplants. *Chin. J. Environ. Eng.* **2023**, *17*, 1748–1760.
19. Bagreev, A.; Bandosz, T.J.; Locke, D.C. Pore structure and surface chemistry of adsorbents obtained by pyrolysis of sewage sludge-derived fertilizer. *Carbon* **2001**, *39*, 1971–1979. [CrossRef]
20. Velghe, I.; Carleer, R.; Yperman, J.; Schreurs, S.; D'Haen, J. Characterisation of adsorbents prepared by pyrolysis of sludge and sludge/disposal filter cake mix. *Water Res.* **2012**, *46*, 2783–2794. [CrossRef]
21. Kante, K.; Qiu, J.; Zhao, Z.; Cheng, Y.; Bandosz, T.J. Development of surface porosity and catalytic activity in metal sludge/waste oil derived adsorbents: Effect of heat treatment. *Chem. Eng. J.* **2008**, *138*, 155–165. [CrossRef]
22. Auta, M.; Hameed, B.H. Optimized and functionalized paper sludge activated with potassium fluoride for single and binary adsorption of reactive dyes. *J. Ind. Eng. Chem.* **2014**, *20*, 830–840. [CrossRef]
23. Bandosz, T.J.; Block, K. Effect of pyrolysis temperature and time on catalytic performance of sewage sludge/industrial sludge-based composite adsorbents. *Appl. Catal. B* **2006**, *67*, 77–85. [CrossRef]
24. Chiang, H.L.; Lin, K.H.; Chiu, H.H. Exhaust characteristics during the pyrolysis of $ZnCl_2$ immersed biosludge. *J. Hazard. Mater.* **2012**, *229–230*, 233–244. [CrossRef] [PubMed]
25. Devi, P.; Saroha, A.K. Improvement in performance of sludge-based adsorbents by controlling key parameters by activation/modification: A critical review. *Crit. Rev. Environ. Sci. Technol.* **2016**, *46*, 1704–1743. [CrossRef]
26. Ahmaruzzaman, M. A review on the utilization of fly ash. *Prog. Energy Combust. Sci.* **2010**, *36*, 327–363. [CrossRef]
27. Patra, K.C.; Rautray, T.R.; Nayak, P. Analysis of grains grown on fly ash treated soils. *Appl. Radiat. Isot.* **2012**, *70*, 1797–1802. [CrossRef] [PubMed]
28. Yao, Z.T.; Ji, X.S.; Sarker, P.K.; Tang, J.H.; Ge, L.Q.; Xia, M.S.; Xi, Y.Q. A comprehensive review on the applications of coal fly ash. *Earth-Sci. Rev.* **2015**, *141*, 105–121. [CrossRef]
29. Temuujin, J.; van Riessen, A.; MacKenzie, K.J.D. Preparation and characterisation of fly ash based geopolymer mortars. *Constr. Build. Mater.* **2010**, *24*, 1906–1910. [CrossRef]
30. Ram, L.C.; Srivastava, N.K.; Jha, S.K.; Sinha, A.K.; Masto, R.E.; Selvi, V.A. Management of lignite fly ash for improving soil fertility and crop productivity. *Environ. Manag.* **2007**, *40*, 438–452. [CrossRef]
31. Lee, S.B.; Lee, Y.B.; Lee, C.H.; Hong, C.O.; Kim, P.J.; Yu, C. Characteristics of boron accumulation by fly ash application in paddy soil. *Bioresour. Technol.* **2008**, *99*, 5928–5932. [CrossRef] [PubMed]
32. Erol, M.; Küçükbayrak, S.; Ersoy-Meriçboyu, A. Characterization of sintered coal fly ashes. *Fuel* **2008**, *87*, 1334–1340. [CrossRef]
33. Wang, S. Application of solid ash based catalysts in heterogeneous catalysis. *Environ. Sci. Technol.* **2008**, *42*, 7055–7063. [CrossRef] [PubMed]
34. Khatri, C.; Mishra, M.K.; Rani, A. Synthesis and characterization of fly ash supported sulfated zirconia catalyst for benzylation reactions. *Fuel Process. Technol.* **2010**, *91*, 1288–1295. [CrossRef]
35. Cho, H.; Oh, D.; Kim, K. A study on removal characteristics of heavy metals from aqueous solution by fly ash. *J. Hazard. Mater.* **2005**, *127*, 187–195. [CrossRef] [PubMed]
36. Hu, J.L.; He, X.W.; Wang, C.R.; Li, J.W.; Zhang, C.H. Cadmium adsorption characteristic of alkali modified sewage sludge. *Bioresour. Technol.* **2012**, *121*, 25–30. [CrossRef] [PubMed]

37. Matheswaran, M.; Karunanithi, T. Adsorption of Chrysoidine R by using fly ash in batch process. *J. Hazard. Mater.* **2007**, *145*, 154–161. [CrossRef] [PubMed]
38. Singh, N. Adsorption of herbicides on coal fly ash from aqueous solutions. *J. Hazard. Mater.* **2009**, *168*, 233–237. [CrossRef]
39. Mao, L.X.; Zhu, S.F.; Wu, M.; Zhao, Q.; Wang, P.C.; Qin, Y.H. Distribution and environmental risk assessment of heavy metals in coal-fired products of power plants. *China Sci.* **2023**, *18*, 1028–1034.
40. Yu, L.; Zhong, Q. Preparation of adsorbents made from sewage sludges for adsorption of organic materials from wastewater. *J. Hazard. Mater.* **2006**, *137*, 359–366. [CrossRef]
41. Gomez-Pacheco, C.V.; Rivera-Utrilla, J.; Sanchez-Polo, M.; Lopez-Penalver, J.J. Optimization of the preparation process of biological sludge adsorbents for application in water treatment. *J. Hazard. Mater.* **2012**, *217–218*, 76–84. [CrossRef]
42. Ping, F.; Chaoping, C.; Dingsheng, C.; Zhixiong, T. Carbonaceous adsorbents prepared from sewage sludge and its application for Hg0 adsorption in simulated flue gas. *Chin. J. Chem. Eng.* **2010**, *18*, 231–238.
43. Kutchko, B.; Kim, A. Fly ash characterization by SEM–EDS. *Fuel* **2006**, *85*, 2537–2544. [CrossRef]
44. Rio, S.; Faur-Brasquet, C.; Le Coq, L.; Courcoux, P.; Le Cloirec, P. Experimental design methodology for the preparation of carbonaceous sorbents from sewage sludge by chemical activationa—-Application to air and water treatments. *Chemosphere* **2005**, *58*, 423–437. [CrossRef] [PubMed]
45. Gascó, G.; Méndez, A.; Gascó, J.M. Preparation of carbon-based adsorbents from sewage sludge pyrolysis to remove metals from water. *Desalination* **2005**, *180*, 245–251. [CrossRef]
46. Hu, Q.; Bin, L.; Li, P.; Fu, F.; Guan, G.; Hao, X.; Tang, B. Highly efficient removal of dyes from wastewater over a wide range of pH value by a self-adaption adsorbent. *J. Mol. Liq.* **2021**, *331*, 115719. [CrossRef]
47. Wei, S.S.; Zhao, Z.Z.; Wu, Y.H.; Liu, H.; Wang, L. Study on adsorption behavior of Cu^{2+} in water by fibrous sepiolite adsorbent. *Ind. Water Treat.* **2022**, *42*, 67–72.
48. El-Azeem, A.; Samy, A.; Ahmad, M.; Usman, A.R.; Kim, K.-R.; Oh, S.-E.; Lee, S.S.; Ok, Y.S. Changes of biochemical properties and heavy metal bioavailability in soil treated with natural liming materials. *Environ. Earth Sci.* **2013**, *70*, 3411–3420. [CrossRef]
49. Chen, T.; Zhou, Z.; Xu, S.; Wang, H.; Lu, W. Adsorption behavior comparison of trivalent and hexavalent chromium on biochar derived from municipal sludge. *Bioresour. Technol.* **2015**, *190*, 388–394. [CrossRef]
50. Wongrod, S.; Simon, S.; van Hullebusch, E.D.; Lens, P.N.L.; Guibaud, G. Changes of sewage sludge digestate-derived biochar properties after chemical treatments and influence on As(III and V) and Cd(II) sorption. *Int. Biodeterior. Biodegrad.* **2018**, *135*, 96–102. [CrossRef]
51. Reddad, Z.; Gerente, C.; Andres, Y.; Le Cloirec, P. Adsorption of several metal ions onto a low-cost biosorbent: Kinetic and equilibrium studies. *Environ. Sci. Technol.* **2002**, *36*, 2067–2073. [CrossRef] [PubMed]
52. Feng, N.; Guo, X.; Liang, S.; Zhu, Y.; Liu, J. Biosorption of heavy metals from aqueous solutions by chemically modified orange peel. *J. Hazard. Mater.* **2011**, *185*, 49–54. [CrossRef] [PubMed]
53. Zuo, W.-Q.; Chen, C.; Cui, H.-J.; Fu, M.-L. Enhanced removal of Cd(II) from aqueous solution using $CaCO_3$ nanoparticle modified sewage sludge biochar. *RSC Adv.* **2017**, *7*, 16238–16243. [CrossRef]
54. Chen, T.; Zhou, Z.; Han, R.; Meng, R.; Wang, H.; Lu, W. Adsorption of cadmium by biochar derived from municipal sewage sludge: Impact factors and adsorption mechanism. *Chemosphere* **2015**, *134*, 286–293. [CrossRef]
55. Inyang, M.; Gao, B.; Yao, Y.; Xue, Y.; Zimmerman, A.R.; Pullammanappallil, P.; Cao, X. Removal of heavy metals from aqueous solution by biochars derived from anaerobically digested biomass. *Bioresour. Technol.* **2012**, *110*, 50–56. [CrossRef]